The effect of ion doping at different sites on the structure, defects and multiferroic properties of BiFeO$_3$ ceramics

CrossMark

Haiyang Dai, Fengjiao Ye, Zhenping Chen[*], Tao Li, Dewei Liu

School of Physics and Electronic Engineering, Zhengzhou University of Light Industry, Zhengzhou, 450002, China

ABSTRACT

The polycrystalline samples of undoped BiFeO$_3$, Ce doped BiFeO$_3$ (Bi$_{0.9}$Ce$_{0.1}$FeO$_3$) and Zr dpoped BiFeO$_3$ (BiFe$_{0.9}$Zr$_{0.1}$O$_3$) were prepared by rapid liquid phase sintering technique. The effects of A-site substitution with Ce and B-site substitution with Zr on the structure, defects and multiferroic properties of BiFeO$_3$ ceramics were comparative investigated. Undoped and doped BiFeO$_3$ samples are well crystallized in perovskite structure, whilst Ce and Zr doping results in slight distortion in the lattice structure. With Ce and Zr doping, the average grain sizes decrease. Positron annihilation lifetime measurements reveal that there are vacancy-type defects in the three samples, and Bi$_{0.9}$Ce$_{0.1}$FeO$_3$ sample has the maximum open volume and concentration of the vacancy defect among those three samples. Both Ce and Zr doping can improve the leakage current, ferroelectric and magnetic properties, whereas Zr doping exhibited better ability. The better electric properties in BiFe$_{0.9}$Zr$_{0.1}$O$_3$ may be due to the effective reduction of oxygen vacancies, Fe^{2+} and impurity phases by Zr doping. The cause for better magnetic properties in BiFe$_{0.9}$Zr$_{0.1}$O$_3$ sample may be that the insertion of Fe vacancies and nonmagnetically active Zr^{4+} ions in antiferromagnetic Fe sublattice can effectively suppress the spiral spin modulation structure.

© 2017 Elsevier B.V. All rights reserved.

1. Introduction

Multiferroic materials that show ferroelectric (or antiferro-electric) and ferromagnetic (or antiferromagnetic) ordering simultaneously have attracted a great deal of attention because of their fascinating fundamental physics as well as the potential applications in information storage, multistate memories, actuators, transducers, sensors, electrically controlled magnetic devices, microelectronic devices and spintronics devices [1–3]. Among single phase multiferroic materials, BiFeO$_3$ (BFO), with a rhombohedrally distorted perovskite structure, is the most intensively studied material because of its high ferroelectric Curie temperature (*T*c~1100 K) and antiferromagnetic Neel temperature (*T*n~640 K), which makes it most possible for applications at room temperature [3–6].

Although BFO presents outstanding advantages, several crucial problems have hindered the practical application of BFO material to multifunctional devices. These problems include: (i) it is difficult to synthesis single-phase samples because of the metastable state of BFO and the volatilization of Bi$_2$O$_3$ [1,2]; (ii) the leakage current is too high due to the formation of impurity phase, Fe^{2+} ions and oxygen vacancies, which hinders the potentially excellent ferroelectric properties of this material [2–7]; (iii) the magnetic properties in BFO is very weak owing to the cancellation of the possible nonzero remanent magnetization permitted by the canted G-type antiferromagnetic order by the space-modulated spin structure [2–7]. To overcome these problems, a number of attempts have been made. Amongst the various ways of improving the multiferroic properties of BFO, lattice site substitution in BFO with appropriate ion is found to be an economical and effective method [3–7]. A large number of rare earth ions (La^{3+}, Sm^{3+}, Dy^{3+}, Ho^{3+}, Eu^{3+}, etc) and alkaline earth ions (Ca^{2+}, Sr^{2+}, Ba^{2+}, etc) have been used to substitute the Bi site of BFO ceramics, and transition metal ions (Ti^{4+}, Mn^{4+}, Cr^{3+}, Ta^{5+}, etc) have been used to substitute its Fe site [1–7]. The ionic radius of Ce^{4+} is closer to that of Bi^{3+}, and the ionic radius of Zr^{4+} is similar to that of Fe^{3+}, therefore, Ce^{4+} and Zr^{4+} ions were suitable for substitution at Bi and Fe sites, respectively. Especially, the substitution of Ce^{4+} for Bi^{3+} and Zr^{4+} for Fe^{3+} in BFO requires charge compensation, leading to the filling of oxygen vacancies and the creation of cation vacancies. Consequently, the multiferroic properties of BFO can be influenced greatly by Ce^{4+} and Zr^{4+} doping. Therefore, Ce^{4+} substitution for Bi and Zr^{4+}

substitution for Fe^{3+} seem especially attractive. In BFO, since the ferroelectric behavior comes from the $6s^2$ lone pair electrons of Bi^{3+} while the magnetic behavior arises mainly from the partially filled 3d orbital of Fe^{3+} [8], the influences of ion doping at different sites on the electric and magnetic properties of BFO ceramics might be different. However, the effect of ion doping at different sites on the structure and multiferroic of BFO has rarely been reported [9,10]. In addition, vacancies are the dominant point defects in perovskite oxide and can dramatically change the physical properties of the materials [11]. Therefore, the study of defects in perovskite oxide is benefit for understanding the structural origin of physical properties. In this paper, A-site Ce and B-Site Zr doped BFO samples were prepared by rapid liquid phase sintering technique, and the influences of ion doping at different sites on the structure, defects and multiferroic properties of BFO ceramics were investigated.

2. Experimental details

Undoped BFO, $Bi_{0.9}Ce_{0.1}FeO_3$ and $BiFe_{0.9}Zr_{0.1}O_3$ compounds were synthesized by rapid liquid phase sintering technique. High purity starting powders of Bi_2O_3 (99.999%), CeO_2 (99.99%), Fe_2O_3 (99.99%) and ZrO_2 (99.99%) were used and exactly weighed according to the stoichiometric ratio with 3% excess of Bi_2O_3 for compensation of Bi loss. The reasons for selecting 3% Bi_2O_3 excess are as follows: The addition of excess Bi to compensate for bismuth loss had been reported in some literature [12–16], and the addition amount of excess Bi is often less than 5%. In our previous experiments, the effects of excess Bi_2O_3 (0%, 3% and 5%) on the structure and properties of BFO have been investigated. The results indicated that the sample with 0% Bi_2O_3 excess had many Bi-poor phase $Bi_2Fe_4O_9$, the sample with 5% Bi_2O_3 excess had a certain amount of Bi-rich phase $Bi_{25}FeO_{39}$, while the sample with 3% Bi_2O_3 excess could form single phase or has a small amount of $Bi_2Fe_4O_9$ due to the phase composition of BFO were sensitive to preparation parameters. Meanwhile, the multiferroic properties of sample with 3% Bi_2O_3 excess were best. Therefore, 3% Bi_2O_3 excess had been selected in this paper. The starting powders were thoroughly ground in an agate mortar for 6 h using ethanol as a medium. The mixed powders were dehydrated at 150 °C for 12 h and dry pressed into small discs with 11 mm in diameter and 1.5 mm in thickness at 10 MPa pressure. The pressed disks were directly put into a furnace at temperature of 850−880 °C and sintered for 30 min in air, they then were taken out of the furnace immediately and quenched subsequently to room temperature naturally. After sintering, the disks were polished and coated with silver paste on both sides and then dried in oven at 600 °C for 30 min before taking electrical measurements.

The sintered pellets were ground and X-ray powder diffraction data were collected in the range of 20°−60° with a 2θ step of 0.02° using a Bruker D8 X-ray diffractometer with Cu-Ka radiation (λ = 0.1541 nm) at room temperature. The microstructure of the samples was observed by scanning electron microscopy (SEM, FEI Quanta200). The positron annihilation lifetime spectra were measured at room temperature (20 ± 0.5 °C) using a fast−fast coincidence lifetime spectrometer. A ^{22}Na positron source with intensity of about 13 μ Ci was used. The positron source was sandwiched between two identical pieces of samples for the positron lifetime measurements. Each spectrum contained a total of 10^6 counts. All the lifetime spectra were analyzed by PATFIT program. The leakage current and ferroelectric properties of all samples were measured using a RT 6000 ferroelectric tester. Magnetization versus applied magnetic field (M-H) data were collected at room temperature in applied magnetic fields of up to 70 kOe using a vibrating-sample magnetometer (VSM) integrated in a physical property measurement system (PPMS, Quantum Design).

3. Results and discussion

Fig. 1 shows XRD patterns of the undoped BFO, $Bi_{0.9}Ce_{0.1}FeO_3$ and $BiFe_{0.9}Zr_{0.1}O_3$ samples. All prepared samples are fully crystallized, since intense peaks are evident. The main diffraction peaks of all samples are matched with those of rhombohedral structure with a space group of $R3c$ [5–8]. Some low intensity diffraction peaks of impurity phases ($Bi_2Fe_4O_9$, marked by *) are detected in the XRD pattern of undoped BFO [4–6]. The occurrence of those phases is unavoidable during the kinetics of BFO formation due to Bi volatilization [1,14,17]. It is interesting to note that the impurity peaks in $Bi_{0.9}Ce_{0.1}FeO_3$ is reduced as compared with the undoped BFO, while no impurity phases can be observed in XRD patterns of $BiFe_{0.9}Zr_{0.1}O_3$. It means that the doping of Ce^{4+} ions at A-site is beneficial to suppress the formation of impurity phases, and the doping of Zr^{4+} ions at B-site in BFO can eliminate the impurity phases and yield single phases. Since the valance of Ce^{4+} and Zr^{4+} is higher than that of Bi^{3+} and Fe^{3+} ions, respectively, the Ce^{4+} ion substituting Bi^{3+} ion and Zr^{4+} ion substituting Fe^{3+} ion acts as a donor in BFO. The addition of Ce^{4+} or Zr^{4+} ion requires charge compensation which can be achieved by suppression of oxygen vacancies, thus resulting in the restrained reduction of Fe^{3+} to Fe^{2+}. Therefore, Ce and Zr doping can suppress or eliminate the formation of impurity phases. The expanded pattern of the peak around 22.5° is plotted in the inset of Fig. 1. It can be seen that the introduction of Ce ions shifts slightly the diffraction peak position toward higher diffraction angle side as compared to the undoped BFO, while the addition of Zr ions shifts slightly the diffraction peak position toward lower diffraction angle side. The shift of diffraction peak position indicates that the Ce and Zr ions are getting substituted into BFO lattice and induce structural distortion. The lattice parameters for the undoped BFO, $Bi_{0.9}Ce_{0.1}FeO_3$ and $BiFe_{0.9}Zr_{0.1}O_3$ are listed in Table 1. On the basis of the best fit to data, it is found that the structure of all samples is rhombohedral, which means that the crystal structure of the samples is unchanged after Ce and Zr doping. From the data it can also be found that the lattice parameters slightly decrease for Ce-doped BFO, but they slightly increase for Zr-doped BFO, which may be mainly attributed to the fact that the ionic radius of Ce^{4+} (0.87 Å) is smaller than that of Bi^{3+} (1.03 Å) but the ionic radius of Zr^{4+} (0.72 Å) is larger than that of Fe^{3+} (0.64 Å) [18].

The scanning electron micrograph of undoped BFO, $Bi_{0.9}Ce_{0.1}FeO_3$ and $BiFe_{0.9}Zr_{0.1}O_3$ samples are presented in Fig. 2. It can be found that the grain size of undoped BFO is significantly higher
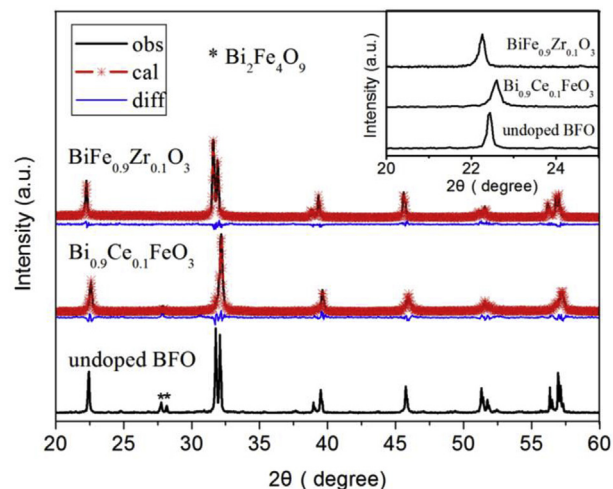

Fig. 1. XRD patterns of the undoped BFO, $Bi_{0.9}Ce_{0.1}FeO_3$ and $BiFe_{0.9}Zr_{0.1}O_3$ samples.